Food Chemistry 346 (2021) 128893

Contents lists available at ScienceDirect

Food Chemistry

journal homepage: www.elsevier.com/locate/foodchem

Target specific aptamer-induced self-assembly of fluorescent graphene quantum dots on palladium nanoparticles for sensitive detection of tetracycline in raw milk

Syed Rahin Ahmed, Satish Kumar, Greter A. Ortega, Seshasai Srinivasan *, Amin Reza Rajabzadeh *

School of Engineering Practice and Technology, McMaster University, 1280 Main Street West Hamilton, Ontario L8S 4L7, Canada

ARTICLE INFO

Keywords:
Tetracyclines detection
GQDs
Pd NPs
Aptasensor
Biosensor
Fluorescence assay

ABSTRACT

The excessive use of tetracyclines (TCs), a bacteriostatic antibiotic, in food products, has led to the accumulation of TCs residues in the human body, affecting human health seriously. Therefore, the development of a highly sensitive method to detect TCs in food is of utmost importance. This study reports a novel sensing strategy using aptamer-induced fluorescence fluctuation of graphene quantum dots (GQDs) and palladium nanoparticles (Pd NPs) for the rapid and label-free detection of tetracycline with a limit of detection of 45 ng.mL^{-1}. A novel single-step synthesis of positively charged Pd NPs and one-step green synthesis of GQDs directly from graphite has been developed. The proposed strategy provides an efficient way to detect low traces of TCs and a new technique for the development of aptamer-based sensors.

1. Introduction

Tetracycline (TC) is a common antibiotic extensively used in the prevention and treatment of bacterial diseases as it provides effective antibacterial properties with minimal side effects. Moreover, TC is used as a feed additive in the agriculture sector for promoting animal growth (de Faria, Rosa, Silveira, & Figueiredo, 2017; Granados-Chinchilla, Rodríguez, Antonio, & Avila, 2017; Granados, Thangarasu, Singh, & Vázquez-Ramos, 2019). The excessive use of this antibiotic in the dairy farm, for example, could cause its concentration to reach above the maximum residue limit (MRL) in milk, which may cause adverse health effects, such as diarrhea, white patches inside the mouth or on lips, upset stomach or loss of appetite if accumulating in the human body through the food chain (Jalalian, Karimabadi, Ramezani, Abnous, & Taghdisi, 2018; Jia et al., 2019; X. Liu et al., 2018). Hence, sensitive detection of TCs in food products is urgently needed for the protection of human health. A literature review shows that various methods of TCs detection has been reported using high-performance liquid chromatography (Lai et al., 2020; Vargas Mamani, Reyes Reyes, & Rath, 2009; Xu et al., 2016), mass spectrometry (Jiang et al., 2020; Moreno-González & García-Campaña, 2017), and capillary electrophoresis (Wu, Xu, Huang, & Shao, 2016). However, all these approaches are time-consuming, expensive, and require sophisticated laboratory equipment and highly trained personnel. Although the colorimetric detection methods do not need advanced laboratory equipment or highly trained staff, unfortunately, the methods suffer from low sensitivity and long detection time, making it challenging for practical uses (Abedalwafa, Li, Ni, & Wang, 2019).

In recent years, fluorescent materials have gained huge research interest in the field of biosensing due to their reliability and reproducibility (J. Song et al., 2018; Sun, Wang, & Lei, 2015). In particular, the applications of nanostructured fluorescent materials over organic dye in biosensing have increased significantly due to their emission stability and ease of preparation in aqueous media (Wolfbeis, 2015). Among different fluorescent nanomaterials, the series of cadmium semiconductor nanocrystals have shown superiority in the following: (i) stability in different media for a wide range of pH values; (ii) detection sensitivity in bioassay systems; (iii) detection response; (iv) optical properties; and (v) bioconjugation ability (Ahmed et al., 2020). Despite several advantages, cadmium semiconductor nanocrystals are toxic, which limits their application in the bio-related field and the environmental assay (Mo et al., 2017; Ranjbar-Navazi, Omidi, Eskandani, & Davaran, 2019; Sandroni et al., 2018). To overcome the problems associated with cadmium nanocrystals, GQDs with superior

* Corresponding authors.
E-mail addresses: ssriniv@mcmaster.ca (S. Srinivasan), rajaba@mcmaster.ca (A.R. Rajabzadeh).

https://doi.org/10.1016/j.foodchem.2020.128893
Received 12 July 2020; Received in revised form 6 November 2020; Accepted 13 December 2020
Available online 30 December 2020

biocompatibility and adjustable emission properties have emerged as promising materials in biosensing (Fasbender et al., 2019; M. Li, Chen, Gooding, & Liu, 2019; Tian, Tang, Teng, & Lau, 2018; Yan et al., 2019; Zhou, Zou, Tran, & Lee, 2015). GQDs have a high surface to volume ratio, which allows them to bind to more target biomolecules and, consequently, enhance detection sensitivity. Furthermore, GQDs have unique conductivity and optical properties, making them highly suitable for optical and electrochemical biosensors. GQDs could easily bind to biomolecules through either covalent or noncovalent bindings (π-π interaction and electrostatic interaction) (Wang, Wu, & Wei, 2018).

To date, several methods for the synthesis of GQDs using bottom-up and top-down approaches have been reported. In general, the bottom-up approaches are superior to top-down since these methods allow to prepare uniform-sized QDs with adjustable optical properties. Some of the bottom-up methods for the synthesis of GQDs include the hydrothermal method (Xie, Lai, & Huq, 2017), plasma treatment (Z. Li et al., 2016; D. Liu et al., 2018), electrochemical approach (Ahirwar, Mallick, & Bahadur, 2017), and microwave synthesis (W. Li et al., 2018; Singh, Kumar, Singh, Savu, & Moshkalev, 2019). However, in most of the published articles, researchers employ graphene oxide (GO) as a precursor material, which is derived from pristine graphite. The conversion of graphite to GO requires a substantial amount of chemicals and strong acids and is a time-consuming process. Currently, few researchers have reported the production of GQDs directly from graphite; however, the methods are either multi-steps or require sophisticated equipment (Table S1). To overcome these drawbacks, a novel single-step method to synthesize GQDs directly from graphite using L-ascorbic acid, which has mild reductive ability and is nontoxic, is reported in this study. This study follows a simple bottom-up approach to synthesize monodispersed water-soluble blue-emissive GQDs with the assistance of ascorbic acid.

Recent studies have revealed that Pd NPs are ideal energy acceptor candidates for fluorescence resonance energy transfer-based sensors (H. Li, Shi, Sun, Li, & Liu, 2016; H. Li et al., 2017). Pd NPs, are of great research interest because of their catalytic, mechanical, and optical properties, which extend their application to chemical and biochemical sensing (Chen & Ostrom, 2015; Kucherenko, Soldatkin, Kucherenko, Soldatkina, & Dzyadevych, 2019; Yi et al., 2017). Though Pd NPs demonstrates excellent performance in catalytic or electro-catalytic applications, the application of Pd NPs for biosensing of analytes is still elusive (Dumas & Couvreur, 2015).

Aptamer-based biosensors have attracted intense research interest in the food industry, biomedical and environmental analysis since its discovery because of their smaller size compared to traditional antibodies, stability, and cost-effectiveness. In particular, the flexibility of use and manipulation and the ease of structure design make aptamers promising candidates to develop biosensors with high sensitivity and selectivity. Most importantly, the recent advances of nanomaterials and their combination with aptamers bring unprecedented advantages in the sensing performance of aptamer-based sensors (S. Song, Wang, Li, Fan, & Zhao, 2008).

Herein, the sensing mechanism of TCs involves Pd NPs as a fluorescent quencher of GQDs in the presence of TCs specific aptamers. As shown in Fig. 1, the presence of the target TCs enhances the fluorescence emission by releasing the GQDs. As a result, the fluorescence emission is indirectly proportional to the concentration of tetracycline. The proposed TCs sensing strategy does not require any washing step compared to a conventional ELISA-based colorimetric method or any chemical for labeling, which potentially makes the method less expensive than the existing techniques. Moreover, the proposed aptamer-based sensing assay could operate under mild reaction conditions and with a portable fluorescence reader, making it a promising real-life device for TCs detection.

2. Materials & methods

Graphite nanopowder, Palladium (II) chloride ($PdCl_2$), *L*(+)-ascorbic acid, tetracyclines, and 3,3′,5,5′-tetramethylbenzidine (TMB) were purchased from Sigma-Aldrich, USA. All the chemicals were of analytical grade and were used as received without further purification. The sequence of the tetracycline Aptamer (Qi et al., 2018) 5′-CGTACGGAATT CG CTAGCCCCCCGGCAGGCCACGGCTTGGGTTGGTCCCACTGCGCGTGGATCCGAGCTCCACGTG-3′) was purchased from Integrated DNA Technologies, USA.

2.1. Synthesis of graphene quantum dots

GQDs were synthesized through a hydrothermal approach using an autoclave. Briefly, 1 mL (0.1 M) of *L*(+)-ascorbic acid and graphite nanopowder (0.1 mg/mL, 15 mL) were mixed in aqueous media and kept in an autoclave at 150 °C for 2 h. The GQDs samples were cooled at room temperature and filtered through a 0.22-μm microporous membrane to remove unreacted graphite. The prepared GQDs solution was yellow. The solution was further dialyzed in a dialysis bag (retained molecular weight: 3,000 to 8,000 Da), and the purified GQDs were separated for further use. Here, *L*(+)-ascorbic acid acts as a reducing agent, and as a stabilizer of QDs.

2.2. Synthesis of palladium nanoparticles

In this study, a new one-step method was developed to synthesize non-spherical Pd NPs using TMB as a reducer and a stabilizer. The solution of Pd NPs was prepared by gently stirring 1.00 mL aqueous

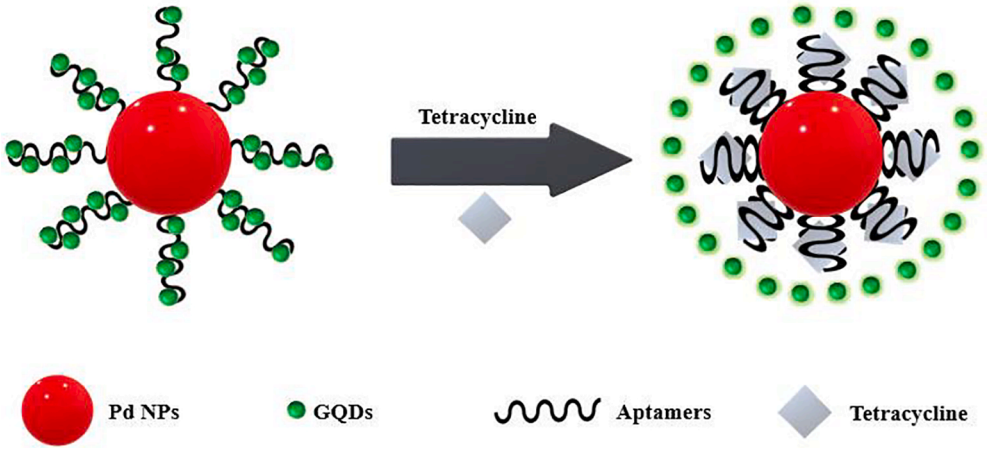

Fig. 1. Schematic presentation of the experimental design of TCs detection.

solution of $PdCl_2$ with 100 μL of TMB (0.1 mg mL^{-1}) solution at room temperature for 10 min. The initial light-yellow color of the $PdCl_2$ solution turned dark brown, indicating the formation of Pd NPs. As-synthesized Pd NPs solution was centrifuged three times at 15,000 rpm for 30 min, and the purified residue of Pd NPs was redispersed in deionized water (DI water) for further use.

2.3. Conjugation of aptamer with Pd NPs

The aptamer was dissolved in 1.00 mL DI water (18.2 MΩ cm), heated to 95 °C for 3 min, and cooled to room temperature to form single-stranded structures. Briefly, 1.00 mL of the synthesized Pd NPs solution was mixed with a serious of 2, 4, 6, 8, 10, 12, 14, & 16 μM (20 μL) aptamer solution separately (diluted with PBS buffer, pH 7.5), and the mixture was gently stirred for 60 min at room temperature. The NPs were conjugated with the aptamers through electrostatic interactions. The conjugated Pd NPs/aptamers were separated from their unconjugated parts through centrifugation at 5000 rpm for 30 min, and the residue was redispersed in 1 mL of Milli-Q water. Dynamic light scattering (DLS) was performed to study zeta potential and to confirm the conjugation of Pd NPs/aptamer.

2.4. Conjugation of GQDs with Pd NPs/aptamer

The conjugation between GQDs and Pd NPs/aptamer was performed through π–π stacking interaction (Y. Liu, Yan, Okoth, & Zhang, 2015). Briefly, 0.2 mL of the Pd NPs/aptamer solution was mixed with 0.8 mL of the GQDs solution, and the mixture was gently stirred for 3 h at room temperature. The mixture was centrifuged at 3000 rpm for 30 min to separate the conjugated Pd NPs/aptamer/GQDs from the free GQDs and Pd NPs/aptamer in the supernatant.

2.5. General procedure of fluorescent biosensing of TCs

The stock solution (50 μL) of varying concentrations of TC were added into the wells of a microplate containing 80 μL of Pd NPs/aptamers/GQDs solution and gently mixed for 5 min at room temperature. The resulting solution (130 μL) was used directly for the fluorescence emission measurement using a fluorescence spectrophotometer.

2.6. Detection of TCs in spiked raw milk samples

The practical applicability of the proposed TCs assay was investigated in spiked milk samples. The TCs stock solutions of 50, 60, 70, 80, 90, and 100 ng.mL^{-1} were prepared with commercial milk samples (Neilson dairy milk, Saputo Inc., Georgetown, Ontario, Canada). The prepared TCs stock solutions (50 μL) were added into each well of a 96 well microtiter plate containing 80 μL of Pd NPs/aptamers/GQDs solution. The 96 well microtiter plate was gently mixed for 5 min at room temperature. The resulting solution (130 μL) was used for the fluorescence emission measurement using a fluorescence microplate reader.

2.7. Spectroscopy and structural characterization

The ultraviolet–visible (UV–Vis) spectra and fluorescence emission were measured using a BioTEK fluorescence spectrophotometer. The microscopic structure of the nanomaterials was characterized using a transmission electron microscope (TEM, (FEI Tecan G2 F20, Oregon, USA) and a high-resolution transmission electron microscope (HR-TEM, Titan 80–300 LB, Oregon, USA). Fluorescence lifetime (τ) of GQDs was measured at a 380-nm excitation wavelength using a light-emitting diode (LED; PTI Inc., Oakland, CA, USA).

2.8. The limit of detection calculation

The limit of detection (LOD) value was calculated based on standard deviation method, i.e., three times the standard deviation of blank absorbance (n = 10) divided by the slope of the regression equation:

$LOD = (3.SD)/m$ where SD and m indicate the standard deviation of the mean blank signal, and the slope of the linear regression curve, respectively.

3. Results and discussion

3.1. Principle of analytical assay

The biosensing method presented in this article is based on two strategies: A) π–π stacking interaction between the GQDs and aptamers, and B) the interaction between TCs and aptamers specific to TCs. It is well known that the interaction between the aptamer and its target TCs is highly specific compared to the interaction between aptamer/GQDs, which is typically nonspecific and weak. The sensitivity of the biosensor reduces if the interaction between aptamer/GQDs is stronger than that of aptamer/TCs. The electrostatic interaction in Pd NPs/aptamer conjugates and π-π interaction in aptamer/GQDs conjugates bring Pd NPs and GQDs in close proximity, which facilitates the fluorescence quenching of the fluorophore. The loose binding of aptamer/GQDs conjugates breaks and releases the GQDs in the presence of target TCs, allowing the fluorescence emission to increase. As a result, the fluorescence emission is directly proportional to the release of GQDs and indirectly proportional to the concentration of TCs.

3.2. Spectroscopic and microscopic studies of GQDs and Pd NPs

Fluorescence spectroscopy of the as-synthesized GQDs exhibited excitation and emission peak located at 335 nm and 435 nm, respectively (Figs. S1 & 2A). The microscopic study using TEM images showed that prepared GQDs were well-distributed, and the average size of GQDs was 1.5–3 nm (Fig. 2B). The homogeneously dispersed solution of GQDs allowed the fluorescence emission from GQDs, thereby helping increase the sensitivity of the biosensor. In this sense, the synthesized GQDs is a suitable candidate to develop a sensitive fluorescence biosensor. The High-Resolution TEM image of the GQDs solution in Fig. 2C showed the lattice fringes with an interplanar distance of 0.33 nm corresponding to (0 0 6) diffraction plane of graphitic carbon (JCPDS 26-1076) (Kumawat, Thakur, Gurung, & Srivastava, 2017). The synthesized GQDs solution appeared blue under UV light irradiation, whereas it was deep yellow in daylight (Fig. 2D). The fluorescence quantum yield, which is the ratio of the photons absorbed to those emitted through fluorescence, was calculated as 6.7%. The production yield of GQDs was 48%. Table S1 compares the proposed synthesis method in this study with reported methods for the synthesis of GQDs directly from graphite. As seen in Table S1, the proposed single-step method for the direct synthesis of GQDs from graphite is simpler than other reported approaches, requires fewer chemicals, and can be done in a short time. This method can therefore be employed in several practical applications that require large-scale production of water-soluble blue emissive GQDs.

The UV–visible spectrum of the synthesized Pd NPs revealed a broad spectrum range from 250 nm to 400 nm, as shown in Fig. 3A. Such a broad spectrum range allows quenching a large range of fluorescence emissions, which is desirable in the proposed biosensing approach. The TEM image of Pd NPs showed that the particles had an average size of approximately 60 nm. Interestingly, the shape of Pd NPs revealed a non-spherical form with some spike on the surface (Fig. 3B & 3C). In general, spiky nanostructures demonstrate an improved biosensing performance due to the large surface-to-volume ratio. The surface charge of synthesized Pd NPs was +40 eV due to the amino group of TMB capped on it. The positive charge on Pd NPs enables to conjugate easily with antibodies or aptamer through electrostatic forces without a need for crosslinkers, which potentially lowers the production cost and effort.

The formation of Pd NPs/aptamers/GQDs conjugation was confirmed through zeta potential measurement. As shown in Table S2,

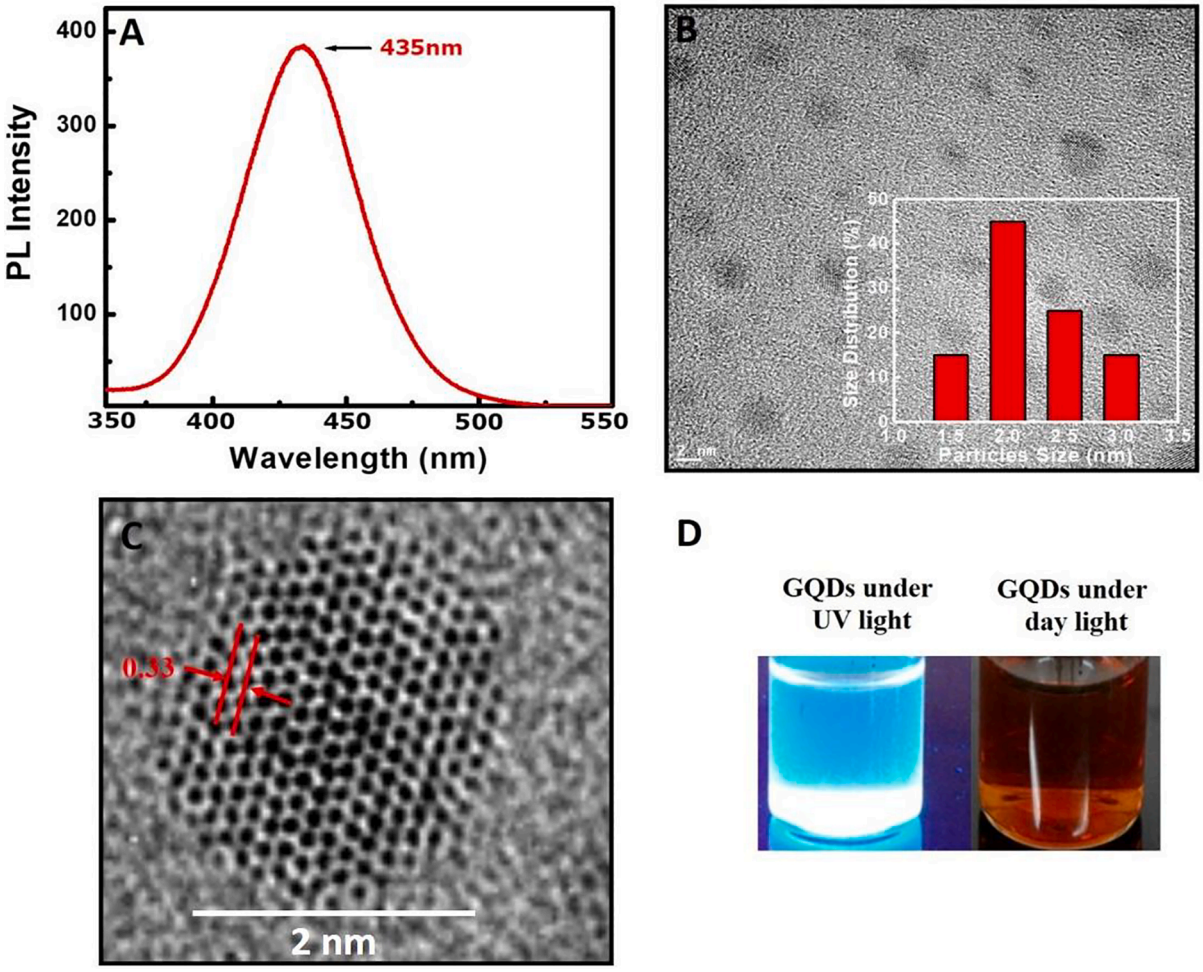

Fig. 2. Characterisation of GQDs: (A) fluorescence emission spectrum of GQDs; (B) TEM (inset: the size distribution of GQDs) and HRTEM image of GQDs (C) and (D) the corresponding color of GQDs under UV and daylight.

the synthesized Pd NPs acquired a positive charge of +40 eV. The surface charge dropped to −1.3 eV when the Pd NPs was conjugated with the negatively charged aptamer. The surface charge further decreased from −1.3 eV to −20 eV when the Pd NPs/aptamer was conjugated with the GQDs. Fig. 4A shows that the fluorescence intensity of GQDs in Pd NPs/aptamers/GQDs conjugate was approximately 55% lower than the fluorescence intensity of the free GQDs, confirming the successful conjugation of Pd NPs/aptamers/GQDs.

A series of experiments to optimize the concentration aptamer and Pd NPs/aptamer were performed, and the results are shown in Figs. S2 and S3. The optimized concentrations of aptamer and Pd NPs/aptamer were 10 μM and 0.2 mL, respectively. Moreover, the performance of the biosensor was optimized by evaluating the effect of the incubation time and the volume of Pd NPs/aptamers/GQDs conjugates. As shown in Fig. S4, 5 min reaction time (Fig. S4A) and 80 μL of Pd NPs/aptamers/GQDs conjugates resulted in the highest fluorescence emission intensity once mixed with 50 μL of the target TCs (100 ng.mL^{-1}) (Fig. S4B). After optimized all the necessary steps, various concentration solutions of TCs in PBS buffer (pH 7.5) were prepared and added to the 80 μL of Pd NPs/aptamers/GQDs conjugate solutions. The fluorescence intensity of the prepared solutions was measured after 5 min for different concentration ranges of the target TCs. Fig. 4B and 4C illustrate the photoluminescence (PL) intensity of TCs at the concentration ranges of 100–500 ng.mL^{-1} and 40–90 ng.mL^{-1}, respectively. The results show that the spectroscopic responses of Pd NPs/aptamers/GQDs conjugate depend on the concentration of TCs in the sample. The higher the concentration of TCs on the Pd NPs/aptamers/GQDs conjugate, the higher the release of GQDs and, consequently, the higher the spectroscopic responses (PL intensity). The results in Fig. 4D reveals a sharp linear increase with TCs concentration in the concentration range of 40–90 ng.mL^{-1}. The correlation coefficient and LOD were calculated as 0.9925 and 18 ng.mL^{-1}, respectively. The results confirm the high sensitivity of the proposed method for the detection of low concentration of TCs. At TCs concentrations higher than 100 ng.mL^{-1}, the fluorescence intensity increased with a milder slope than that at the lower concentrations of TCs. The milder slope is due to the steric hindrance and self-quenching of GQDs, which commonly occur at the high concentration of analytes in the fluorescence techniques.

To investigate the reproducibility of the proposed TCs biosensor, ten samples of Pd NPs/aptamer/GQDs conjugated solution (80 μL) were placed in different wells of a microplate and 40 ng.mL^{-1} of aptamer solution (50 μL) were added to each well. The fluorescence intensity of each sample was measured, and the results were summarized in Fig. S5. The results show a mean PL intensity of 100 with a standard deviation of ± 4, indicating the high reproducibility of the proposed detection strategy. Furthermore, the stability of the TCs biosensor was examined by checking the fluorescence intensity of Pd NPs/aptamers/GQDs conjugates for a period of 15 days. Fig. S6 shows that the fluorescence signal (PL intensity) remained within a range of 99 ± 3 (mean ± standard deviation) for 15 days. The detection time of the proposed sensor was compared with some other recent reports. As shown in Table S3, the detection time in the present study (5 min) is less compared to other reported methods (10–95 min). The fluorescence lifetime of GQDs was also measured before and after adding target TCs, and the results are

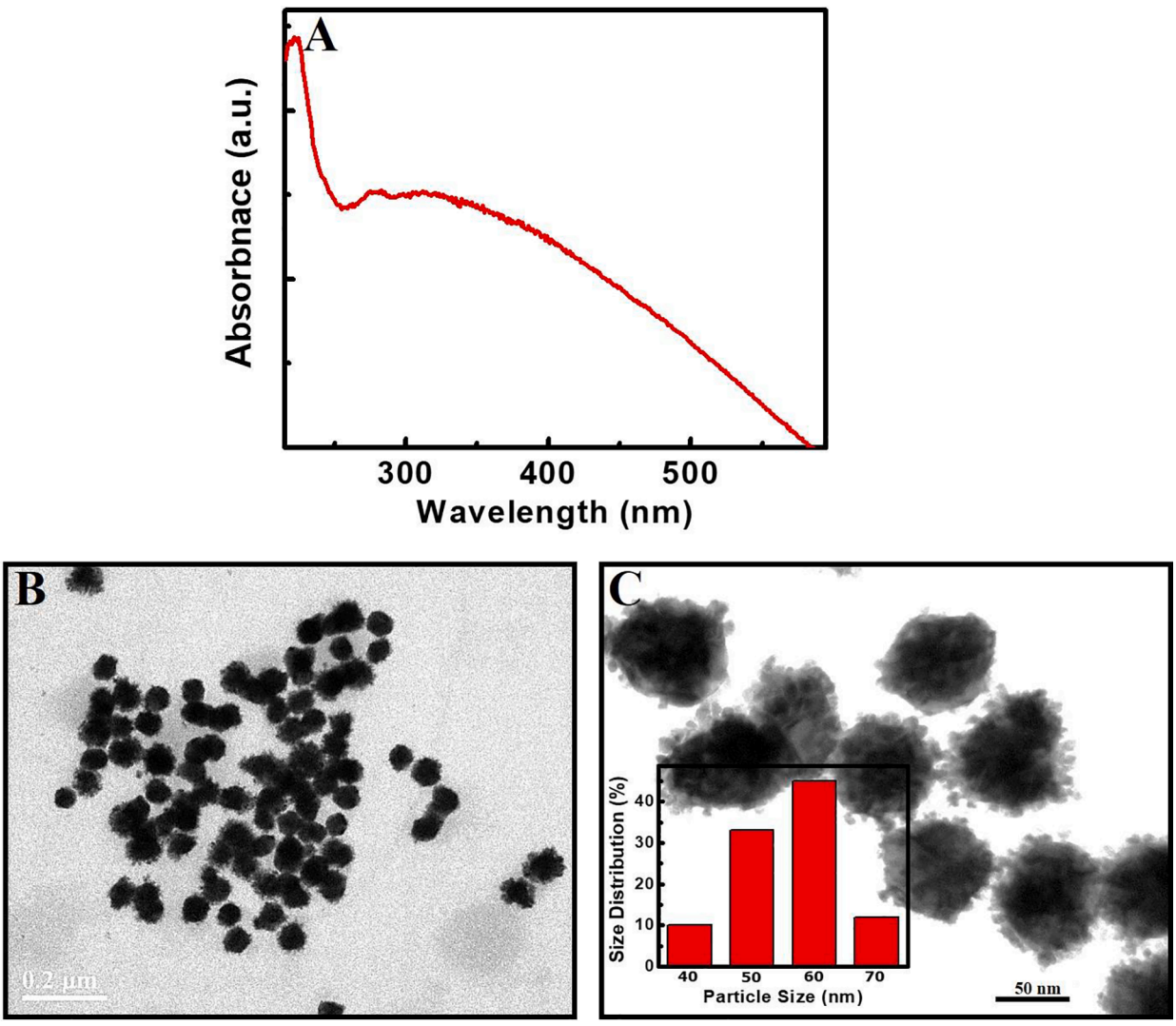

Fig. 3. Characterisation of Pd NPs: (A) Absorbance spectrum of Pd NPs; (B) Far view TEM image of Pd NPs; and (C) Close view TEM image of Pd NPs (inset: the size distribution of Pd NPs).

shown in Fig. S7. The fluorescence lifetime of synthesized GQDs was 3.9 ns. A significant change of lifetime (1.9 ns) was observed for Pd NPs/aptamers/GQDs conjugates, most probably due to the fluorescence resonance energy transfer at close proximity of Pd NPs. After adding target TCs (100 ng.mL^{-1}), the fluorescence lifetime of synthesized GQDs was 2.5 ns indicating the release of GQDs from the Pd NPs/aptamers/GQDs conjugates.

The selectivity of Pd NPs/aptamer/GQDs conjugates towards TCs was investigated by measuring the fluorescence intensity of 80 μL of Pd NPs/aptamers/GQDs conjugates exposed to 50 μL (500 ng.mL^{-1}) of various antibiotics. As can be seen from Fig. 5A, the Pd NPs/aptamer/GQDs conjugates in the presence of other antibiotics such as gramicidin (Gm), amoxicillin (Ax), azithromycin (Ar), and erythromycin (Er) showed minimal change in the fluorescence intensity compared to the fluorescence intensity of the conjugates in the absence of antibiotics. On the other hand, upon the introduction of TCs to Pd NPs/aptamer/GQDs conjugates, the emission of GQDs was significantly enhanced. These results demonstrated the high selectivity of the proposed method for the detection of TCs.

The feasibility of the proposed strategy was assessed on TCs spiked raw milk samples. As shown in Fig. 5B, the linear response of TCs detection in the raw milk samples was up to 60 ng.mL^{-1}, and the LOD was calculated as 45 ng.mL^{-1}.

For validating the performance of the proposed strategy for the detection of TCs, the recovery of TCs in spiked raw milk samples were evaluated. The milk samples were spiked with TCs at four different concentrations (40, 60, 80, and 100 ng.mL^{-1}). As shown in Table 1, the recovery of TCs by the aptasensor was in the range of 98.37–107.9% with the relative standard deviation, RSD, of less than 4%. These results confirm the reliability and high accuracy of the proposed strategy and provide great potential for sensitive, specific, and convenient detection of TCs in real samples.

4. Conclusion

In this study, an aptamer-based fluorescence assay for ultrasensitive detection of TCs was developed. Some of the novel features of this study include 1) single-step synthesis of positively charged Pd NPs; 2) one-step green synthesis of GQDs directly from graphite; and 3) simple development of an aptasensor for rapid and label-free fluorescence-based detection of TCs with a LOD of 45 ng.mL^{-1} in raw milk samples has been presented. The proposed synthesis and sensing strategy would overcome the drawbacks of the existing methodologies by lowering the manufacturing costs of nanomaterials (single-step synthesis of Pd NPs and direct synthesis of GQDs from graphite) and allowing for rapid and high sensitive detection of TCs without a need for sophisticated

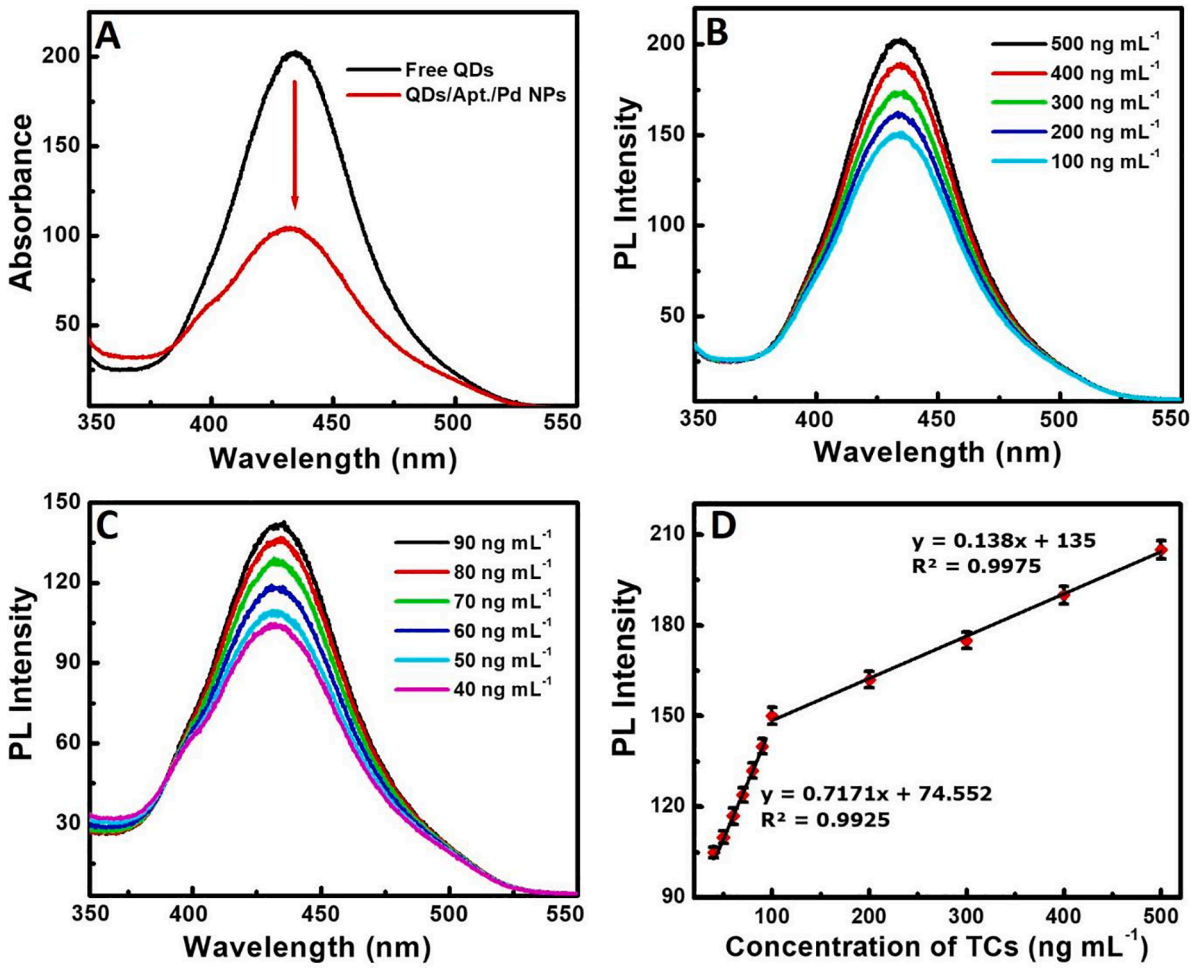

Fig. 4. Analytical performance of the proposed method: (A) quenching comparison of Pd NPs/aptamer/GQDs with free GQDs (apt. means aptamers); (B) sensing of TCs at a concentration range of 100–500 ng.mL^{-1}; (C) sensing of TCs at a concentration range of 40–90 ng.mL^{-1}& (D) the calibration curve of TCs vs. PL intensity.

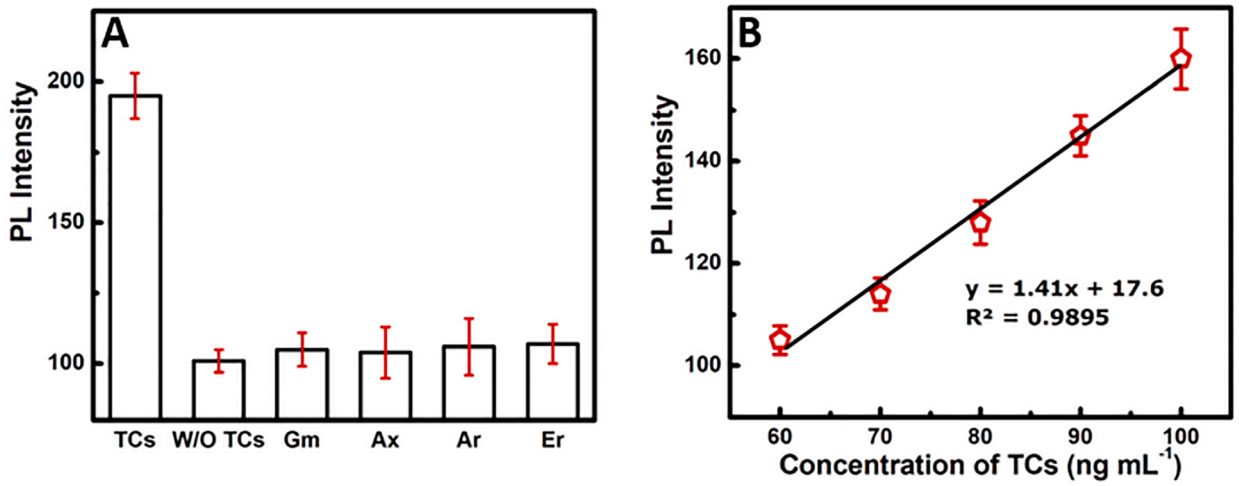

Fig. 5. Selectivity of proposed TCs detection in the presence of tetracycline (TCs), gramicidin (Gm), amoxicillin (Ax), azithromycin (Ar) and erythromycin (Er) (A). W/O TCs represents the Pd NPs/Aptamer/GQDs in the absence of TCs and other antibiotics; (B) the detection results of TCs in spiked milk samples.

instruments. The concept of the sensing strategy reported in this study could be applied to other target biomolecules by changing the aptamer. Thus, the proposed bioassay would be a universal platform for the development of efficient aptasensors in different fields.

CRediT authorship contribution statement

Syed Rahin Ahmed: Investigation, Formal analysis, Methodology, Writing - original draft. **Satish Kumar:** Investigation, Writing - review & editing. **Greter A. Ortega:** Investigation, Writing - review & editing.

Table 1
Precision (relative standard deviation, RSD%) and recovery study of the TCs from milk samples.

TCs Added (ng.mL^{-1})	TCs found (ng.mL^{-1})	RSD (%, N = 3)	Recovery (%)
0	ND	ND	
40	39.5	3.7	98.75
60	60.6	2.9	101
80	78.7	3.1	98.37
100	107.9	2.4	107.9

ND means Not Detected.

Seshasai Srinivasan: Supervision, Conceptualization, Resources, Writing - review & editing. **Amin Reza Rajabzadeh:** Supervision, Conceptualization, Methodology, Writing - review & editing.

Declaration of Competing Interest

The authors declare that they have no known competing financial interests or personal relationships that could have appeared to influence the work reported in this paper.

Appendix A. Supplementary data

Supplementary data to this article can be found online at https://doi.org/10.1016/j.foodchem.2020.128893.

References

Abedalwafa, M. A., Li, Y., Ni, C., & Wang, L.u. (2019). Colorimetric sensor arrays for the detection and identification of antibiotics. *Analytical Methods, 11*(22), 2836–2854. https://doi.org/10.1039/C9AY00371A.

Ahirwar, S., Mallick, S., & Bahadur, D. (2017). Electrochemical method to prepare graphene quantum dots and graphene oxide quantum dots. *ACS Omega, 2*(11), 8343–8353. https://doi.org/10.1021/acsomega.7b01539.s001.

Ahmed, S. R., Chand, R., Kumar, S., Mittal, N., Srinivasan, S., & Rajabzadeh, A. R. (2020). Recent biosensing advances in the rapid detection of illicit drugs. *TrAC Trends in Analytical Chemistry, 131*, 116006. https://doi.org/10.1016/j.trac.2020.116006.

Chen, A., & Ostrom, C. (2015). Palladium-based nanomaterials: Synthesis and electrochemical applications. *Chemical Reviews, 115*(21), 11999–12044. https://doi.org/10.1021/acs.chemrev.5b00324.

de Faria, H. D., Rosa, M. A., Silveira, A. T., & Figueiredo, E. C. (2017). Direct extraction of tetracyclines from bovine milk using restricted access carbon nanotubes in a column switching liquid chromatography system. *Food Chemistry, 225*, 98–106. https://doi.org/10.1016/j.foodchem.2017.01.004.

Dumas, A., & Couvreur, P. (2015). Palladium: A future key player in the nanomedical field? *Chemical Science, 6*(4), 2153–2157. https://doi.org/10.1039/C5SC00070J.

Fasbender, S., Zimmermann, L., Cadeddu, R.-P., Luysberg, M., Moll, B., Janiak, C., … Haas, R. (2019). The low toxicity of graphene quantum dots is reflected by marginal gene expression changes of primary human hematopoietic stem cells. *Scientific Reports, 9*(1). https://doi.org/10.1038/s41598-019-48567-6.

Granados-Chinchilla, F., Rodríguez, C., Antonio, J., & Avila, R. (2017). Review Article Tetracyclines in Food and Feedingstuffs: From Regulation to Analytical Methods, Bacterial Resistance, and Environmental and Health Implications. doi: 10.1155/2017/1315497.

Granados, J. A. O., Thangarasu, P., Singh, N., & Vázquez-Ramos, J. M. (2019). Tetracycline and its quantum dots for recognition of Al3+ and application in milk developing cells bio-imaging. *Food Chemistry, 278*, 523–532. https://doi.org/10.1016/j.foodchem.2018.11.086.

Jalalian, S. H., Karimabadi, N., Ramezani, M., Abnous, K., & Taghdisi, S. M. (2018). Electrochemical and optical aptamer-based sensors for detection of tetracyclines. *Trends in Food Science & Technology, 73*, 45–57. https://doi.org/10.1016/j.tifs.2018.01.009.

Jia, P., Bu, T., Sun, X., Liu, Y., Liu, J., Wang, Q., … Wang, L.i. (2019). A sensitive and selective approach for detection of tetracyclines using fluorescent molybdenum disulfide nanoplates. *Food Chemistry, 297*, 124969. https://doi.org/10.1016/j.foodchem.2019.124969.

Jiang, T., Peng, Z., Xie, M., Fang, X., Hong, Y.i., Huang, Z., … Zhu, Z. (2020). Rapid analysis of tetracycline in honey by microwave plasma torch mass spectrometry with ablation samples. *Analytical Methods, 12*(4), 535–543. https://doi.org/10.1039/C9AY01887E.

Kucherenko, I. S., Soldatkin, O. O., Kucherenko, D. Y., Soldatkina, O. V., & Dzyadevych, S. V. (2019). Advances in nanomaterial application in enzyme-based electrochemical biosensors: A review. *Nanoscale Advances, 1*(12), 4560–4577. https://doi.org/10.1039/C9NA00491B.

Kumawat, M. K., Thakur, M., Gurung, R. B., & Srivastava, R. (2017). Graphene quantum dots for cell proliferation, nucleus imaging, and photoluminescent sensing applications. *Scientific Reports, 7*(1), 1–16. https://doi.org/10.1038/s41598-017-16025-w.

Lai, X., Liu, J., Xu, X., Li, J., Zhang, B., Wei, L., Cai, H., … Cheng, X. (2020). Ultrasensitive high-performance liquid chromatography determination of tetracycline antibiotics and their 4-epimer derivatives based on dual effect of methanesulfonic acid. *Journal of Separation Science, 43*(2), 398–405. https://doi.org/10.1002/jssc.201900618.

Li, H., Shi, L., Sun, D.-e., Li, P., & Liu, Z. (2016). Fluorescence resonance energy transfer biosensor between upconverting nanoparticles and palladium nanoparticles for ultrasensitive CEA detection. *Biosensors and Bioelectronics, 86*, 791–798. https://doi.org/10.1016/j.bios.2016.07.070.

Li, H., Yang, D., Li, P., Zhang, Q., Zhang, W., Ding, X., … Wu, J. (2017). Palladium nanoparticles-based fluorescence resonance energy transfer aptasensor for highly sensitive detection of aflatoxin M1 in milk. Toxins, 9(10). doi: 10.3390/toxins9100318.

Li, M., Chen, T., Gooding, J. J., & Liu, J. (2019). Review of carbon and graphene quantum dots for sensing. *ACS Sensors, 4*(7), 1732–1748. https://doi.org/10.1021/acssensors.9b00514.s001.

Li, W., Li, M., Liu, Y., Pan, D., Li, Z., Wang, L., & Wu, M. (2018). Three minute ultrarapid microwave-assisted synthesis of bright fluorescent graphene quantum dots for live cell staining and white LEDs. *ACS Applied Nano Materials, 1*(4), 1623–1630. https://doi.org/10.1021/acsanm.8b00114.s001.

Li, Z., Li, Z., Wu, Y., Nan, J., Wang, H., Zhang, X., … Yang, B. (2016). Tuning the bandgap of graphene quantum dots by gold nanoparticle-assisted O2 plasma etching. *RSC Advances, 6*(100), 97853–97860. https://doi.org/10.1039/C6RA16409A.

Liu, D., Chen, X., Hu, Y., Sun, T., Song, Z., Zheng, Y., … Wei, D. (2018). Raman enhancement on ultra-clean graphene quantum dots produced by quasi-equilibrium plasma-enhanced chemical vapor deposition. *Nature Communications, 9*(1). https://doi.org/10.1038/s41467-017-02627-5.

Liu, X., Huang, D., Lai, C., Zeng, G., Qin, L., Zhang, C., … Zhang, Y. (2018). Recent advances in sensors for tetracycline antibiotics and their applications. *TrAC Trends in Analytical Chemistry, 109*, 260–274. https://doi.org/10.1016/j.trac.2018.10.011.

Liu, Y., Yan, K., Okoth, O. K., & Zhang, J. (2015). A label-free photoelectrochemical aptasensor based on nitrogen-doped graphene quantum dots for chloramphenicol determination. *Biosensors and Bioelectronics, 74*, 1016–1021. https://doi.org/10.1016/j.bios.2015.07.067.

Mo, D., Hu, L., Zeng, G., Chen, G., Wan, J., Yu, Z., … Cheng, M. (2017). Cadmium-containing quantum dots: Properties, applications, and toxicity. *Applied Microbiology and Biotechnology, 101*(7), 2713–2733. https://doi.org/10.1007/s00253-017-8140-9.

Moreno-González, D., & García-Campaña, A. M. (2017). Salting-out assisted liquid–liquid extraction coupled to ultra-high performance liquid chromatography–tandem mass spectrometry for the determination of tetracycline residues in infant foods. *Food Chemistry, 221*, 1763–1769. https://doi.org/10.1016/j.foodchem.2016.10.107.

Qi, M., Tu, C., Dai, Y., Wang, W., Wang, A., & Chen, J. (2018). A simple colorimetric analytical assay using gold nanoparticles for specific detection of tetracycline in environmental water samples. *Analytical Methods, 10*(27), 3402–3407. https://doi.org/10.1039/C8AY00713F.

Ranjbar-Navazi, Z., Omidi, Y., Eskandani, M., & Davaran, S. (2019). Cadmium-free quantum dot-based theranostics. *TrAC Trends in Analytical Chemistry, 118*, 386–400. https://doi.org/10.1016/j.trac.2019.05.041.

Sandroni, M., Gueret, R., Wegner, K. D., Reiss, P., Fortage, J., Aldakov, D., & Collomb, M.-N. (2018). Cadmium-free CuInS 2 /ZnS quantum dots as efficient and robust photosensitizers in combination with a molecular catalyst for visible light-driven H 2 production in water. *Energy & Environmental Science, 11*(7), 1752–1761. https://doi.org/10.1039/C8EE00120K.

Singh, R. K., Kumar, R., Singh, D. P., Savu, R., & Moshkalev, S. A. (2019). Progress in microwave-assisted synthesis of quantum dots (graphene/carbon/semiconducting) for bioapplications: A review. *Materials Today Chemistry, 12*, 282–314. https://doi.org/10.1016/j.mtchem.2019.03.001.

Song, J., Zhou, H., Gao, R., Zhang, Y., Zhang, H., Zhang, Y., … Zhao, H. (2018). Selective determination of Cr(VI) by glutaraldehyde cross-linked chitosan polymer fluorophores. *ACS Sensors, 3*(4), 792–798. https://doi.org/10.1021/acssensors.8b00038.s001.

Song, S., Wang, L., Li, J., Fan, C., & Zhao, J. (2008). Aptamer-based biosensors. *TrAC – Trends in Analytical Chemistry, 27*(2), 108–117. https://doi.org/10.1016/j.trac.2007.12.004.

Sun, X., Wang, Y., & Lei, Y.u. (2015). Fluorescence based explosive detection: From mechanisms to sensory materials. *Chemical Society Reviews, 44*(22), 8019–8061. https://doi.org/10.1039/C5CS00496A.

Tian, P., Tang, L., Teng, K. S., & Lau, S. P. (2018). Graphene quantum dots from chemistry to applications. *Materials Today Chemistry, 10*, 221–258. https://doi.org/10.1016/j.mtchem.2018.09.007.

Vargas Mamani, M. C., Reyes Reyes, F. G., & Rath, S. (2009). Multiresidue determination of tetracyclines, sulphonamides and chloramphenicol in bovine milk using HPLC-DAD. *Food Chemistry, 117*(3), 545–552. https://doi.org/10.1016/j.foodchem.2009.04.032.

Wang, L.i., Wu, A., & Wei, G. (2018). Graphene-based aptasensors: From molecule–interface interactions to sensor design and biomedical diagnostics. *Analyst, 143*(7), 1526–1543. https://doi.org/10.1039/C8AN00081F.

Wolfbeis, O. S. (2015). An overview of nanoparticles commonly used in fluorescent bioimaging. *Chemical Society Reviews, 44*(14), 4743–4768. https://doi.org/10.1039/C4CS00392F.

Wu, X., Xu, Z., Huang, Z., & Shao, C. (2016). Large volume sample stacking of cationic tetracycline antibiotics toward 10 ppb level analysis by capillary electrophoresis

with UV detection: CE and CEC. *Electrophoresis, 37*(22), 2963–2969. https://doi.org/10.1002/elps.201600189.

Xie, J.-D., Lai, G.-W., & Huq, M. M. (2017). Hydrothermal route to graphene quantum dots: Effects of precursor and temperature. *Diamond and Related Materials, 79*, 112–118. https://doi.org/10.1016/j.diamond.2017.08.014.

Xu, J.-J., An, M., Yang, R., Tan, Z., Hao, J., Cao, J., … Cao, W. (2016). Determination of tetracycline antibiotic residues in honey and milk by miniaturized solid phase extraction using chitosan-modified graphitized multiwalled carbon nanotubes. *Journal of Agriculture and Food Chemistry, 64*(12), 2647–2654. https://doi.org/10.1021/acs.jafc.6b00748.s001.

Yan, Y., Gong, J., Chen, J., Zeng, Z., Huang, W., Pu, K., Liu, J., & Chen, P. (2019). Recent advances on graphene quantum dots: from chemistry and physics to applications. *Advanced Materials, 31*(21), 1808283. https://doi.org/10.1002/adma.201808283.

Yi, X., Wu, Y., Tan, G., Yu, P., Zhou, L., Zhou, Z., Chen, J., Wang, Z., Pang, J., & Ning, C. (2017). Palladium nanoparticles entrapped in a self-supporting nanoporous gold wire as sensitive dopamine biosensor. *Scientific Reports, 7*(1). https://doi.org/10.1038/s41598-017-07909-y.

Zhou, H., Zou, F., Tran, V. T., & Lee, J. (2015). Simultaneous enhancement of Raman scattering and fluorescence emission on graphene quantum dot-spiky magnetoplasmonic supra-particle composite films. *RSC Advances, 5*(99), 81753–81758. https://doi.org/10.1039/C5RA14176A.